



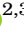




Refinement of the Phase Diagram of the Bi-Te System and the Thermodynamic Properties of Lower Bismuth Tellurides

GUNEL S. HASANOVA ¹, AYTAN I. AGHAZADE ²,
SAMIRA Z. IMAMALIYEVA ², YUSIF A. YUSIBOV ¹,
and MAHAMMAD B. BABANLY ^{2,3}

1.—Ganja State University, 2000 Ganja, Azerbaijan. 2.—Institute of Catalysis and Inorganic Chemistry, ANAS, 1143 Baku, Azerbaijan. 3.—e-mail: babanlymb@gmail.com

Alloys of the system Bi-Te obtained by long-term thermal annealing of samples quenched from 1000 K were studied by differential thermal analysis, x-ray phase diffraction, and scanning electron microscopy methods, as well as by electromotive forces measurements (EMF) of concentration cells relative to a bismuth electrode. A new refined version of the phase diagram which reflects the compounds Bi_2Te_3 , Bi_4Te_5 , Bi_8Te_9 , BiTe, Bi_4Te_3 , Bi_2Te , and Bi_7Te_3 with practically constant compositions was constructed. It was found that all of these compounds, except for Bi_2Te_3 , melt with decomposition by peritectic reactions. Based on powder diffraction patterns, the types and parameters of the crystal lattices of these compounds were determined. The EMF measurements were used to determine the partial molar functions of bismuth in the alloys and the standard integral thermodynamic functions of bismuth tellurides.

INTRODUCTION

Bismuth tellurides with a tetradymite-like layered structure have long been at the center of close attention of researchers as advanced functional materials. These compounds, especially Bi_2Te_3 , solid solutions, doped phases, and composites based on it, have been intensively studied as thermoelectric materials and are used in the manufacture of portable refrigerators, temperature control devices, power generation at space stations, etc.^{1–6} After the discovery of a new quantum state of matter, a topological insulator (TI),^{7,8} it was shown that these phases also exhibit the properties of TI,^{9–15} and are extremely favorable for various applications, including spintronics, quantum computers, medicine, security systems, etc.^{16–18} Moreover, unique optical properties make them promising for use in broadband optoelectronics as photodetectors and switches.^{19–21}

In contrast to Bi_2Te_3 , the functional properties of mixed-layer compounds of the $n\text{Bi}_2\text{mBi}_2\text{Te}_3$ homologous series have been very poorly studied, which is apparently due to the difficulty of obtaining high-quality samples, particularly monocrystals.

The development of methods and optimization of the conditions for the synthesis of compounds and the design of materials based on them, especially in the so-called alloy systems, require reliable data on phase equilibria and thermodynamic properties of the corresponding systems.^{18,22–24}

Despite such an increased interest in bismuth tellurides as the most innovative functional materials, a reliable description of the phase equilibria of this system in the Bi- Bi_2Te_3 region has not yet been established.

According to the phase diagram presented by Hansen and Anderko²⁵ which was built based on the results of many works performed at the beginning of the twentieth century, the Bi-Te system is characterized by the formation of one intermediate phase (β) with congruent melting at 858 K and a homogeneity region of 52–65 at.% Te. It forms eutectics with elemental bismuth and tellurium which crystallize at 539 K and 686 K, respectively. In Ref. 26, these data were basically confirmed and it was

shown that the homogeneity region of the indicated phase covers a wider range of compositions of 32–60 at.% Te (supplementary Fig. S-1a). According to this diagram, the minerals hedleyite (Bi_7Te_3), tsumoite (BiTe), and tellurobismuthite (Bi_2Te_3) already known at that time are included in the β -phase, which was crystallographically incorrect. It was proved that the Bi_2Te_3 compound with congruent melting is outside the homogeneity field of the β -phase and has a narrow (< 1 at %) homogeneity region, while the β -phase is formed by the peritectic reaction $\text{L} + \text{Bi}_2\text{Te}_3 \leftrightarrow \beta$.^{27,28}

In 1958, Abrikosov and Bankina²⁷ presented the second version of the phase diagram (supplementary Fig. S-1b) which was plotted based on DTA results and microstructural analysis of the long-term annealed samples. According to this diagram, in addition to Bi_2Te_3 with congruent melting, there are three compounds, namely Bi_7Te_3 , Bi_2Te , and BiTe , formed by peritectic reactions at 585 K, 693 K, and 813 K, respectively. The last two compounds are phases of variable composition with homogeneity regions of 32.2–36.0 and 45.6–54.7 at.% Te, respectively.

It should be noted that structural studies realized by x-ray phase diffraction (XRD) and electrographic methods demonstrated the existence of a number of layered compounds of the homologous series $n\text{Bi}_2\text{m-Bi}_2\text{Te}_3$.^{29–32} The parameters c of the unit cell of these compounds differed sharply from each other. Taking into account these data, Okamoto and Tenner in 1990 proposed a compiled phase diagram (supplementary Fig. S-1c), in which the compositions of all known and putative (dashed lines) bismuth tellurides were marked.³³ According to Ref. ³⁴, each member of the indicated homologous series has an almost constant composition, since the structural features do not allow the formation of wide homogeneity ranges on their bases. Thus, they indirectly give preference to the phase diagram proposed by Ref. ³³ according to which the system contains compounds of a homologous series with practically constant compositions. However, this diagram is far from being perfect, since it does not indicate the melting (decomposition) temperatures or the natures of most compounds.

In recent years, several works devoted to the experimental study and thermodynamic optimization of the Bi-Te phase diagram have been published.^{35,36} According to the phase diagram (supplementary Fig. S-1d) constructed by Mao et al.³⁵ based on limited experimental data and optimization by the CALPHAD method, in addition to the Bi_2Te_3 compound, there is β -phase with a homogeneity region of 28–52 at.% Te, which transforms into the compounds Bi_2Te (586–616 K) and Bi_4Te_3 (693–713 K); as a result of structural ordering in narrow temperature ranges. In the work of Gierlotka,³⁶ a thermodynamic analysis of the phase

diagram of this system in a more perfect CALPHAD approximation was carried out, and the data of Ref. ³⁵ were confirmed and refined.

In general, thermodynamic properties of bismuth tellurides have been very poorly studied. A literature analysis shows that the data given in modern thermodynamic handbooks and electronic databases,^{37–40} as well as in the original works,^{41–47} refer mainly to the compound Bi_2Te_3 . Only two papers^{40,47} provide the data for the BiTe and Bi_2Te compounds.

Considering all the facts mentioned above, we have undertaken a comprehensive study of phase equilibria in the Bi-Te system and the thermodynamic properties of bismuth tellurides. In our previous work,^{48,49} the data on solid-phase equilibria in the 50–60 at.% Te composition range were presented, the existence of Bi_2Te_3 , Bi_4Te_5 , Bi_8Te_9 , and BiTe compounds with practically constant composition were shown, and their partial and integral thermodynamic functions were determined. This paper presents a refined phase diagram of the Bi-Te system and the results of the thermodynamic study of the compounds Bi_4Te_3 , Bi_2Te , and Bi_7Te_3 .

EXPERIMENTAL

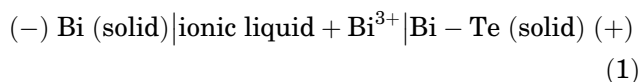
The alloys of the studied system were synthesized by fusing high-purity elemental bismuth and tellurium in evacuated ($\sim 10^{-2}$ Pa) quartz ampoules. When developing the synthesis methodology of samples, we assumed that the bulk samples of layered phases obtained by the widely used fusion method do not reach an equilibrium state even after a long period (2000–3000 h) of thermal annealing.^{1,27,34} This is apparently because, unlike conventional bulk samples, van der Waals phases obtained in non-equilibrium crystallization conditions (i.e., ordinary cooling of the melt) do not practically undergo any changes during further thermal treatment due to very low diffusion between layers.

Taking this into account, to ensure a high dispersion of samples, after alloying, some of them (series I) were quenched by dropping ampoules into ice water from a liquid state (700 K), followed by multi-step annealing. At first, alloys with compositions < 30 at.% Te were annealed at 500 K (1000 h), 32–48 at.% Te at 570 K (1000 h), 50–60 at.% Te at 770 K (1000 h), and then all samples were kept at 370 K for 20 h. For comparison, a number of alloys with selective compositions (series II) were synthesized by the traditional fusion method and annealed under similar conditions.

Studies were carried out by powder x-ray diffraction (PXRD), differential thermal (DTA), scanning electron microscopy (SEM), and electromotive forces (EMF) methods. DTA curves were recorded on a DSC NETZSCH 404 F1 Pegasus system differential scanning calorimeter and a multichannel DTA device based on a TC-08 Thermocouple Data Logger.

Powder diffractograms of the initial compounds and intermediate alloys were recorded using Bruker D8 diffractometer with $\text{CuK}\alpha_1$ radiation in the range of $2\theta = 10\text{--}70^\circ$. The indexing of the PXRD patterns and the refinement of the lattice parameters were implemented by the Topas 4.2 software by the Le Bail method. SEM pictures were taken on a Tescan Vega 3 SBH scanning electron microscope.

For thermodynamic studies by the EMF method, the concentration cells of the type



where assembled and their EMF were measured in the 300–450 K temperature range.

Concentration cells with various liquid and solid electrolytes are widely used for the thermodynamic study of binary and complex metal chalcogenides.^{50–65} When studying metal sulfides and selenides, taking into account the low melting point of elemental sulfur and selenium, it is advisable to carry out measurements at temperatures below the solidus of the corresponding system. For this purpose, the most suitable electrolytes were glycerol solutions of alkali and alkaline earth metals halides.^{51,58–61} In our previous work, we have shown that during such low-temperature measurements, ionic liquids can also be used as an electrolyte.^{64,65} In this work, an ionic liquid (morpholine formate) as an electrolyte was also used. To obtain it, we used morpholine (CAS No.110-91-8), formic acid (CAS No. 64-18-6), and anhydrous BiCl_3 (CAS No.7787-60-2) purchased from Alfa Aesar (Germany). The ionic liquid was obtained according to the method described.⁶⁵

Elementary bismuth was used as the left electrode in the cells of type (1), and the alloys of the series (I) with a composition of 31–48 at.% Te were used as right electrodes. For each phase region, two samples with different compositions were prepared. They served as electrodes in two different cells. The assembly of electrochemical cells of type (1) and the technique of EMF measurements are described in detail in Refs. ⁶⁴ and ⁶⁵.

The first equilibrium EMF values were obtained after keeping the electrochemical cell at ~ 350 K for 40–60 h, followed by every 3–4 h after the establishment of a certain temperature. The EMF values were considered equilibrium if they did not differ from each other upon repeated measurements at a given temperature by more than 0.2 mV, regardless of the direction of the temperature change.

RESULTS AND DISCUSSION

Phase Diagram

The results of the investigation of the series I alloys showed that they are closer to the equilibrium state than samples of series II. In particular, by comparing PXRD patterns with the corresponding

literature data, it was found that the samples with the compositions Bi_2Te_3 , Bi_4Te_5 , Bi_8Te_9 , BiTe , Bi_4Te_3 , and Bi_2Te are single-phase and their diffraction patterns are identical to those given in the literature.

The results of XRD analysis of the alloys in the composition range of 50–60 at.% Te are presented and discussed in Refs. ⁴⁸ and ⁴⁹. The PXRD patterns of some alloys with high bismuth content are shown in Figs. 1 and 2. As can be seen in Fig. 1, alloys with the compositions Bi_4Te_3 and Bi_2Te are single-phase, while the alloy with the composition of Bi_7Te_3 has a slight excess of elemental bismuth and Bi_2Te . We have also defined that the intermediate alloys between the identified compounds are bi-phasic. For example, Fig. 2 shows PXRD patterns of the samples with compositions 32 at.%, 37.5 at.%, and 45 at.% Te, which consist of the two-phase mixtures $\text{Bi}_7\text{Te}_3 + \text{Bi}_2\text{Te}$, $\text{Bi}_2\text{Te} + \text{Bi}_4\text{Te}_3$, and $\text{Bi}_4\text{Te}_3 + \text{BiTe}$, respectively. Note that the absence of other phases in these alloys is an additional feature of their equilibria.

The types and parameters of crystal lattices of bismuth tellurides (supplementary Table S-I), which were determined based on analysis of the diffraction patterns using the Topas 4.2 software and the Le Bail refinement, were in good agreement with the literature.^{4,34,66,67}

The results of the SEM analysis were in accordance with the XRD data. As an example, supplementary Fig. S-2 presents the SEM patterns of alloys of series I with 33.3 at.% and 42.9 at.% Te contents, corresponding to the stoichiometry of Bi_2Te and Bi_4Te_3 , respectively. As can be seen in the figure, both samples are one-phase and have layered structures.

The phase diagram of the Bi-Te system in the 0–60 at.% Te composition range (Fig. 3) was constructed based on the DTA and XRD data. This diagram reflects seven bismuth tellurides, of which Bi_2Te_3 melts congruently at 586°C , while the remaining six compounds melt with decomposition by peritectic reactions (Table I).

Comparison of Fig. 3 with the previously constructed versions of the Bi-Te phase diagram (supplementary Fig. S-1) shows that four compounds (Bi_2Te_3 , BiTe , Bi_2Te , and Bi_7Te_3) indicated in Ref. ²⁷ were confirmed by us. The peritectic decomposition temperatures of the last three compounds differ from the literature data. Moreover, we could not confirm the existence of the wide homogeneity regions in BiTe and Bi_2Te .

The endothermic effects related to the peritectic decomposition reactions of all alloys of series I corresponding to the stoichiometric compositions of incongruently melting compounds were clearly recorded on the heating thermograms.

The DTA heating curves of some samples of the series I are presented in Fig. 4 and series II in the supplementary Fig. S-3, while the cooling curves are presented in supplementary Fig. S-4. As can be

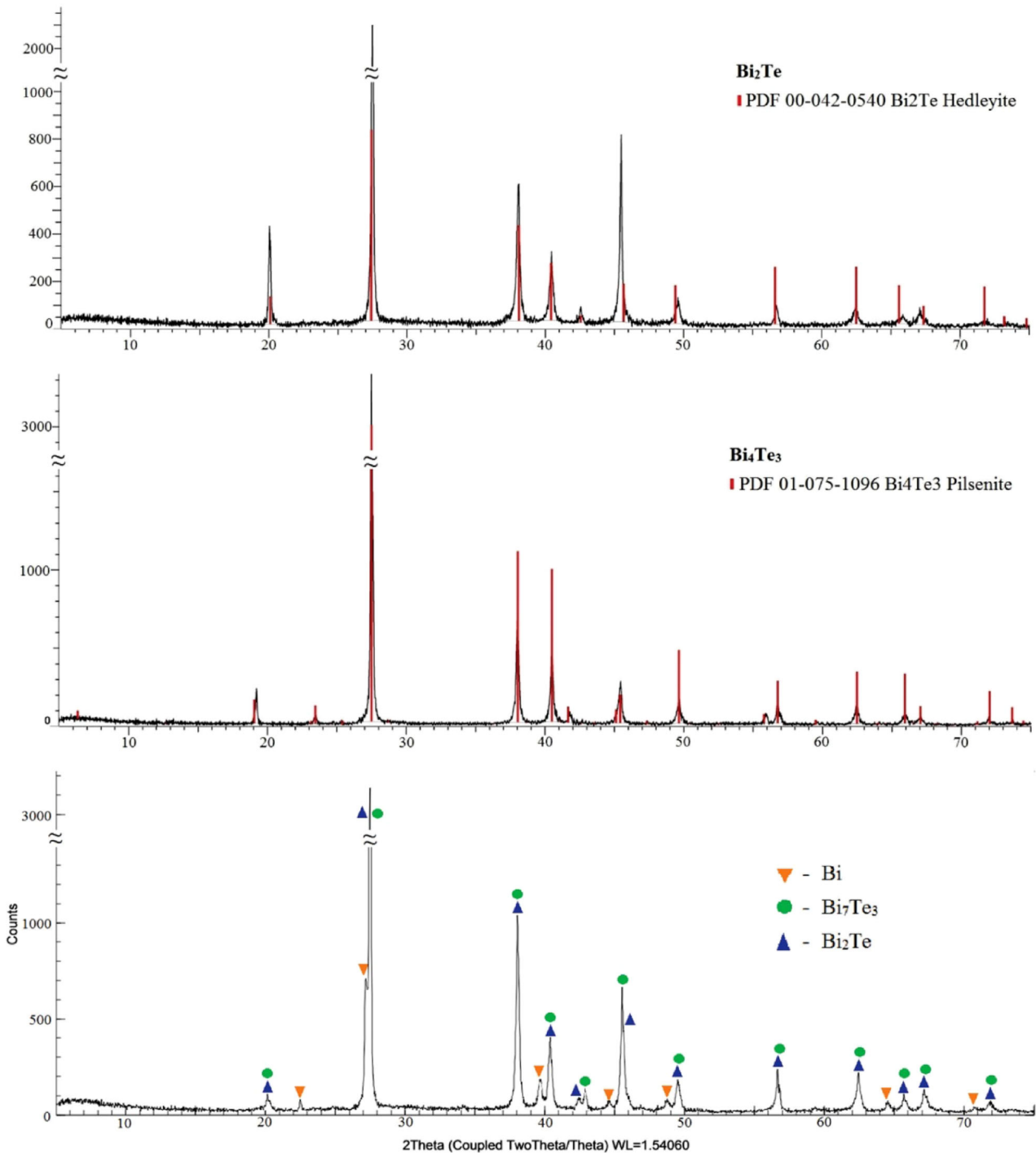


Fig. 1. The powder diffraction pattern of Bi_4Te_3 , Bi_2Te , and Bi_7Te_3 alloys.

seen in Fig. 4, the heating curves for this series of alloys are in good agreement with the T-x diagram in Fig. 3. Five endothermic effects related to the melting of the bismuth-based eutectic (537 K), the peritectic decomposition reactions of Bi_7Te_3 (605 K), Bi_2Te (665 K), Bi_4Te_3 (709 K), and the end of the melting (748 K) were observed on the heating thermogram of the 30-at.% Te composition alloy (Fig. 4a). The presence of a weak endothermic effect

at 537 K indicates the presence of a small amount of elemental bismuth in the sample, which is in agreement with the XRD data (Fig. 1). The DTA heating curve of an alloy with a composition of 40 at.% Te (two-phase region $\text{Bi}_2\text{Te} + \text{Bi}_4\text{Te}_3$) has three endo effects, reflecting the peritectic decomposition reactions of these compounds and the completion of melting (Fig. 4b). Heating thermograms corresponding to the Bi_4Te_3 , BiTe , Bi_8Te_9 ,

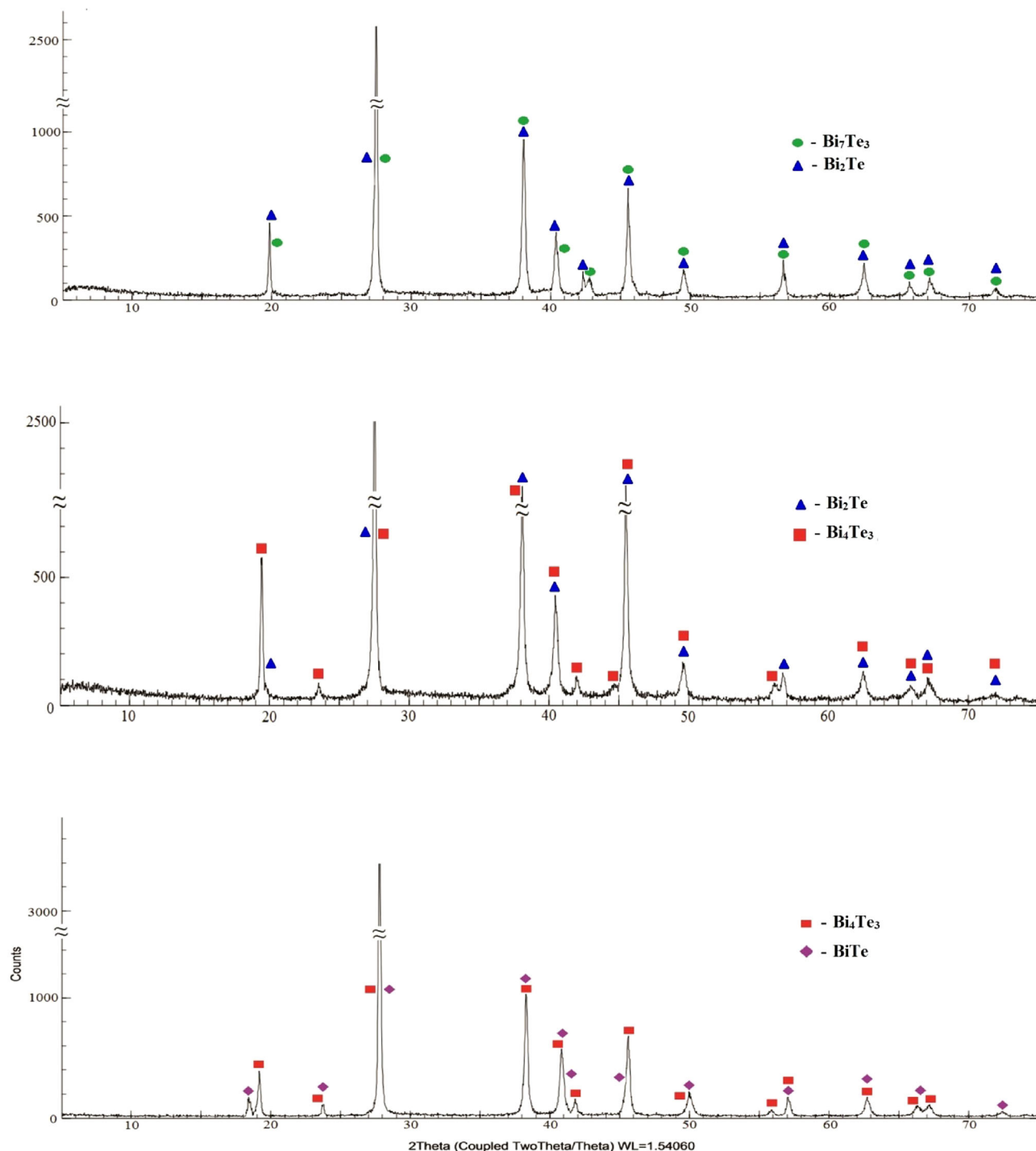


Fig. 2. The powder diffraction pattern of samples of series I with 32 at.%, 37.5 at.% and 45 at.% Te compositions.

and Bi_4Te_5 compounds clearly reflect the peritectic reactions of their decomposition (708 K, 815 K, 823 K, and 835 K) and the completion of melting (Fig. 4c, d, e and f).

The DTA heating curves of samples of series II differed significantly from those for samples of series I. As can be seen in supplementary Fig. S-3, on the thermograms of the samples with the 30 at.% and 40 at.% Te compositions, there are a series of

diffuse endothermic effects in the 538–748 K and 648 the 798 K temperature ranges, and, for an alloy of 50 at.% Te, there is one diffuse endothermic effect. The data of these thermograms are in better agreement with the phase diagrams presented in Refs. ²⁷ and ³⁵ (supplementary Fig. S-1b, d). In particular, the general contours of these curves are close to the data,³⁵ which is interpreted by the authors as the ordering of β -solid solution in narrow

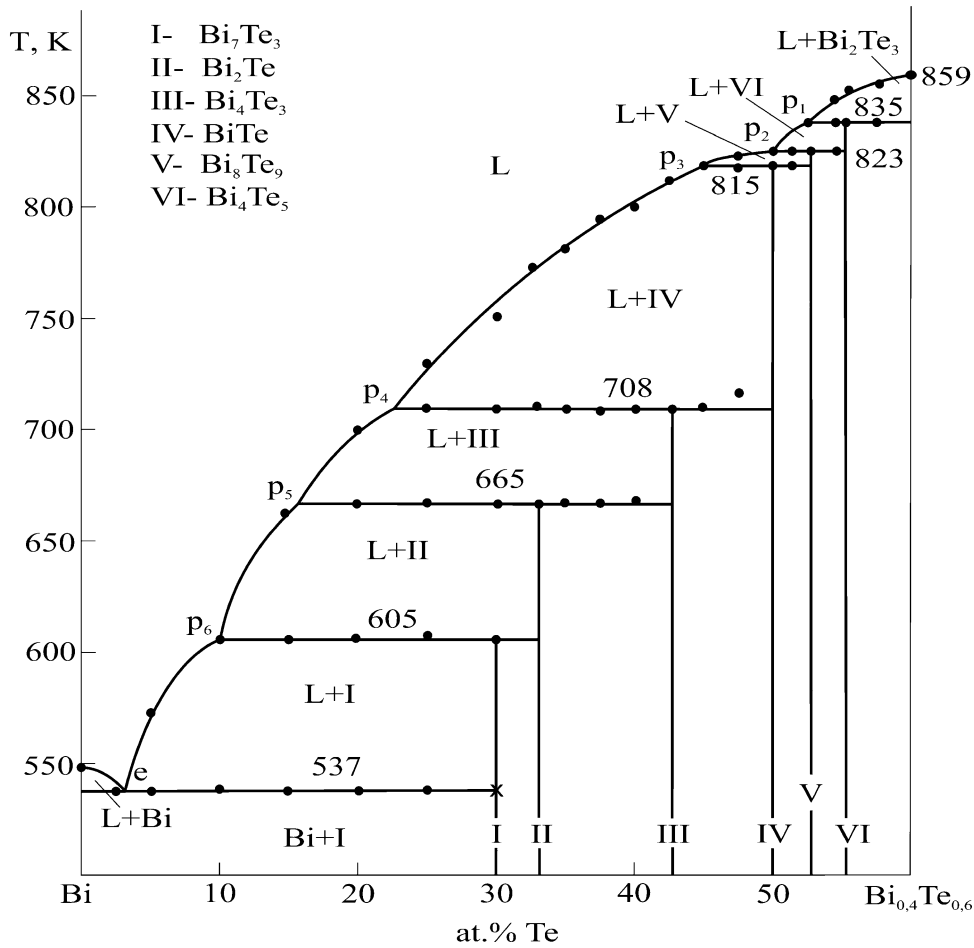


Fig.3. Phase diagram of the Bi-Te system.

Table I. Nonvariant equilibria in the Bi-Bi_{0.4}Te_{0.6} system.

Point in Fig. 3	Equilibria	T (K)	Composition (mol % Te)
P ₁	$\text{L} + \text{Bi}_2\text{Te}_3 \leftrightarrow \text{Bi}_4\text{Te}_5$	835	52
P ₂	$\text{L} + \text{Bi}_4\text{Te}_5 \leftrightarrow \text{Bi}_8\text{Te}_9$	823	50
P ₃	$\text{L} + \text{Bi}_8\text{Te}_9 \leftrightarrow \text{BiTe}$	815	45
P ₄	$\text{L} + \text{BiTe} \leftrightarrow \text{Bi}_4\text{Te}_3$	708	23
P ₅	$\text{L} + \text{Bi}_4\text{Te}_3 \leftrightarrow \text{Bi}_2\text{Te}$	665	16
P ₆	$\text{L} + \text{Bi}_2\text{Te} \leftrightarrow \text{Bi}_7\text{Te}_3$	605	10
E	$\text{L} \leftrightarrow \text{Bi} + \text{Bi}_7\text{Te}_3$	537	2.5

temperature ranges with the formation of Bi_2Te and Bi_4Te_3 compounds.

Valuable information on the nature of the thermal effects on the DTA heating curves (Fig. 4) is provided by their comparison with cooling thermograms. Analysis of the cooling curves (supplementary Fig. S-4) shows that they are identical for the alloys of both series, and are in better agreement with the heating curves of the samples of series II. For example, a comparison of the cooling curve of the 30-at.% Te sample (supplementary Fig. S-4a) with the phase diagram (Fig. 3) shows that the first

exothermic effect (746 K) corresponds to the onset of crystallization, and the subsequent ones correspond to the peritectic reactions of the formation of Bi_4Te_3 (706 K), Bi_2Te (667 K), and the crystallization of the eutectic (536 K). It is interesting that, on the cooling curve of this sample, there are no thermal effects in the temperature range of 583–608 K, recorded on the heating thermograms of the corresponding samples of both series of alloys. It should also be noted that the cooling curve of an alloy of 50-at.% Te composition (supplementary Fig. S-4,c) practically coincides with the heating thermogram of an alloy

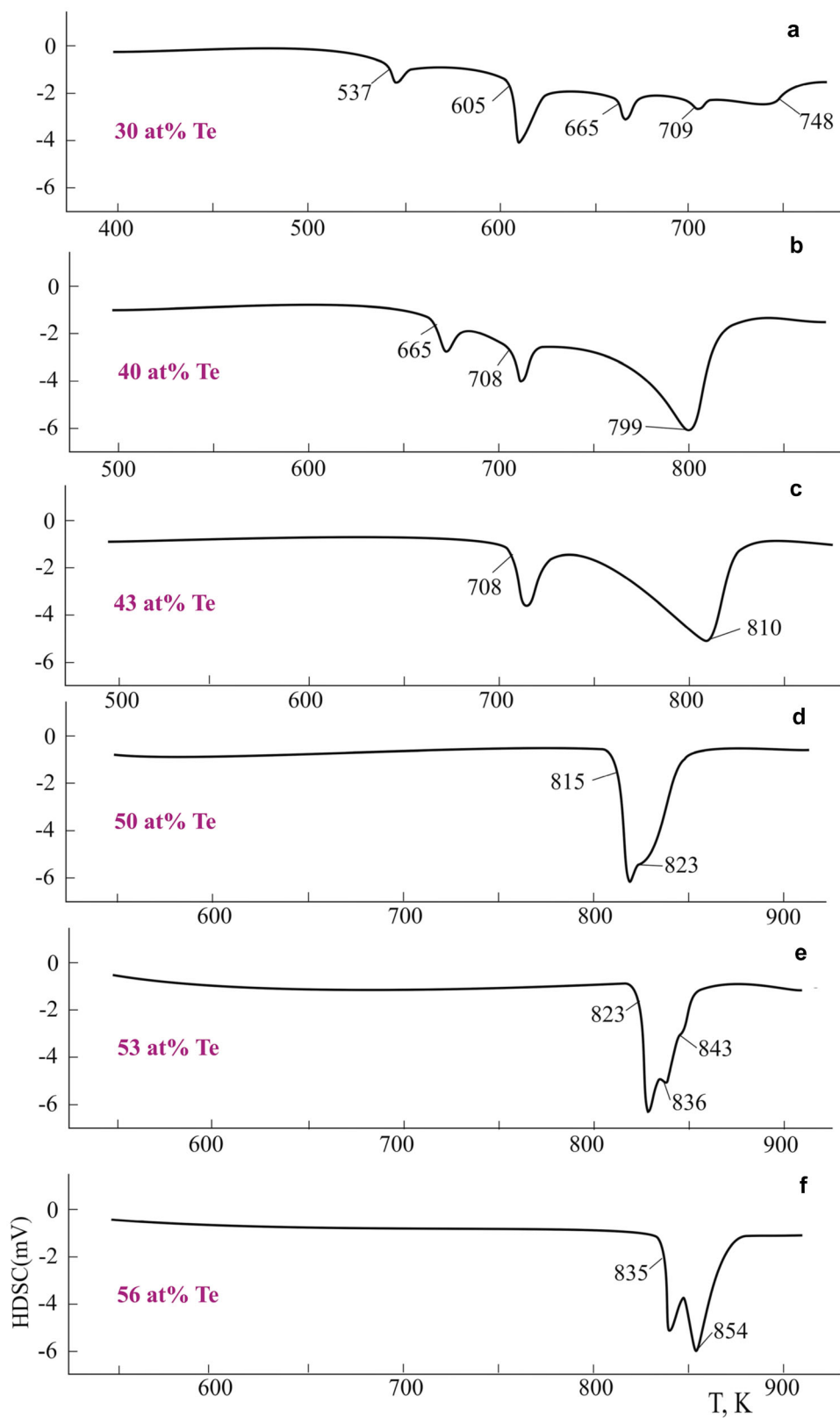


Fig.4. DTA heating curves of some samples of series I.

of the same composition from series II (supplementary Fig. S-3,c).

Thus, a comparison of Fig. 4 with supplementary Figs. S-3 and S-4 shows that the data presented in Fig. 4 are close to equilibrium, and the next two reflect non-equilibrium states and processes. Thermal effects on the cooling curves reflect the series of peritectic formation reactions of the compounds indicated in the phase diagram (Fig. 3). When the melts are cooled, these reactions do not proceed completely and turn into other lower-temperature reactions, including absence from the equilibrium diagram. The closeness of the character of these curves with the heating curves of samples of series II shows that, despite prolonged annealing, they do not reflect an equilibrium state. This confirms the data of Refs. ¹, ²⁷ and ³⁴ on the inefficiency of thermal treatment of alloys of the Bi-Te system.

In summary, 8 out of 15 compounds indicated on the complicated phase diagram³³ have not been confirmed in this work.

Thermodynamic Properties

EMF measurements of cells of type (1) were in accordance with the phase diagram. They had constant values at a given temperature regions on the T-x diagram (Fig. 3), and had linear dependences on temperature (supplementary Fig. S-5). This allows using them for thermodynamic calculations.

The experimental data obtained for alloys in the 31–48 at.% Te compositions range were processed using the Microsoft Office Excel 2003 computer program by the least-squares method. The linear equations obtained are given in Table II in the form recommended in Refs. ⁵¹ and ⁵²

$$E = a + bT \pm t \left[\frac{\delta_E^2}{n} + \delta_b^2 (T - \bar{T})^2 \right]^{1/2} \quad (2)$$

In Eq. 2, a and b are coefficients, n is the number of pairs of E and T values, \bar{T} is the average temperature in K, t Student's t test, and T the temperature in K. δ_E^2 and δ_b^2 are dispersions of individual EMF values and the constant b . Considering the number of experimental points is $n = 30$, at a confidence level of 95%, the Student's test is $t \leq 2$.

From the equations (Table II) using thermodynamic relationships⁵¹

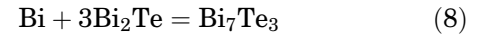
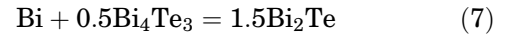
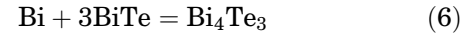
$$\overline{\Delta G}_{\text{Bi}} = -zFE \quad (3)$$

$$\overline{\Delta S}_{\text{Bi}} = zF \left(\frac{\partial E}{\partial T} \right)_P = zFb \quad (4)$$

$$\overline{\Delta H}_{\text{Bi}} = -zF \left[E - T \left(\frac{\partial E}{\partial T} \right)_P \right] = -zFa \quad (5)$$

the partial molar Gibbs free energy, enthalpy, and entropy of bismuth in alloys were calculated (Table III).

These partial molar quantities are thermodynamic functions of the following potential formation reactions (the state of substances is crystalline):^{51,52}



From Eqs. 6, 7, and 8 according to the expressions:

$$\Delta_f Z^0(\text{Bi}_4\text{Te}_3) = \Delta \bar{Z}_{\text{Bi}} + 3\Delta_f Z^0(\text{BiTe}) \quad (9)$$

$$\Delta_f Z^0(\text{Bi}_2\text{Te}) = \frac{2}{3} \Delta \bar{Z}_{\text{Bi}} + \frac{1}{3} \Delta_f Z^0(\text{Bi}_4\text{Te}_3) \quad (10)$$

$$\Delta_f Z^0(\text{Bi}_7\text{Te}_3) = \Delta \bar{Z}_{\text{Bi}} + 3\Delta_f Z^0(\text{Bi}_2\text{Te}) \quad (11)$$

the standard Gibbs free energy and the enthalpy of formation were calculated while using relationships:

$$S^0(\text{Bi}_4\text{Te}_3) = \Delta \bar{S}_{\text{Bi}} + S^0(\text{Bi}) + 3S^0(\text{BiTe}) \quad (12)$$

$$S^0(\text{Bi}_2\text{Te}) = \frac{2}{3} \Delta \bar{S}_{\text{Bi}} + \frac{2}{3} S^0(\text{Bi}) + \frac{1}{3} S^0(\text{Bi}_4\text{Te}_3) \quad (13)$$

$$S^0(\text{Bi}_7\text{Te}_3) = \Delta \bar{S}_{\text{Bi}} + S^0(\text{Bi}) + 3S^0(\text{Bi}_2\text{Te}) \quad (14)$$

Table II. Temperature dependencies of the EMF of the cells type (1) for alloys of the Bi-Te system in the 300–450 K temperature range.

Phase area	$E, \text{mV} = a + bT \pm t \cdot S_E(T)$
$\text{Bi}_4\text{Te}_3\text{-BiTe}$	$43.41 + 0.0290T \pm 2 \left[\frac{0.27}{30} + 4.5 \cdot 10^{-6} (T - 376.38)^2 \right]^{1/2}$
$\text{Bi}_2\text{Te-Bi}_4\text{Te}_3$	$30.39 + 0.0358T \pm 2 \left[\frac{0.22}{30} + 3.7 \times 10^{-6} (T - 376.38)^2 \right]^{1/2}$
$\text{Bi}_7\text{Te}_3\text{-Bi}_2\text{Te}$	$10.71 + 0.0627T \pm 2 \left[\frac{0.21}{30} + 3.4 \times 10^{-6} (T - 376.38)^2 \right]^{1/2}$

Table III. Relative partial molar functions of bismuth in the alloys of the Bi-Te system at 298 K.

Phase area	$-\overline{\Delta G}_{\text{Bi}}$ (kJ mol ⁻¹)	$-\overline{\Delta H}_{\text{Bi}}$ (kJ mol ⁻¹)	$\overline{\Delta S}_{\text{Bi}}$ (J mol ⁻¹ K ⁻¹)
Bi ₄ Te ₃ -BiTe	15.069 ± 0.074	12.56 ± 0.31	8.40 ± 0.82
Bi ₂ Te-Bi ₄ Te ₃	11.889 ± 0.067	8.80 ± 0.28	10.37 ± 0.74
Bi ₇ Te ₃ -Bi ₂ Te	8.515 ± 0.065	3.10 ± 0.27	18.16 ± 0.72

Table IV. Standard integral thermodynamic functions of bismuth tellurides at 298 K.

Compound	$-\Delta_f G^0(298 \text{ K})(\text{kJ mol}^{-1})$	$-\Delta_f H^0(298 \text{ K})(\text{kJ mol}^{-1})$	$S^0(298 \text{ K})(\text{J mol}^{-1} \text{ K}^{-1})$
Bi ₇ Te ₃	150.1 ± 0.7	135.4 ± 2.1	594.2 ± 9.6
Bi ₂ Te	47.2 ± 0.2	44.1 ± 0.6	173.1 ± 2.8
		35.15 ± 2.640	
Bi ₄ Te ₃	117.7 ± 0.7	114.6 ± 1.2	385.2 ± 5.3
Bi ₈ Te ₉ ⁹	268.2 ± 1.5	286.8 ± 2.3	897.0 ± 12.0
BiTe ⁴⁹	34.2 ± 0.2	34.0 ± 0.3	106.7 ± 1.3
Bi ₄ Te ₅ ⁴⁸	147.8 ± 0.8	149.2 ± 1.1	469.7 ± 6.2
Bi ₂ Te ₃ ⁴⁸	76.9 ± 0.2	79.2 ± 0.5	254.2 ± 3.0

the standard entropies of bismuth tellurides were determined. The data obtained are shown in Table - IV. In the calculations, we used the data of³⁷ on the standard entropy of bismuth (56.7 ± 0.5 J mol⁻¹ K⁻¹) and tellurium (49.50 ± 0.21 J mol⁻¹ K⁻¹), as well as the standard integral thermodynamic functions of BiTe.⁴⁹ Errors were determined by the error accumulation method.

In addition to the results of the present study, our data for other bismuth tellurides are given in Table IV.^{48,49} A detailed comparative analysis of our data with references for the Bi₂Te₃ and BiTe compounds is given in Refs. ⁴⁸ and ⁴⁹. It can be seen from Table IV that our data on the enthalpy of formation of Bi₂Te are slightly higher than the value given in Ref. ⁴⁰.

CONCLUSION

We have presented a new set of mutually consistent data on phase equilibria and thermodynamic properties of the Bi-Te system, obtained by DTA, XRD, SEM, and EMF methods. The constructed phase diagram reflects the Bi₂Te₃, Bi₄Te₅, Bi₈Te₉, BiTe, Bi₄Te₃, Bi₂Te, and Bi₇Te₃ compounds with almost constant compositions. It was found that Bi₂Te₃ melts congruently at 859 K, and the rest melt with peritectic reactions at 835, 823, 815, 708, 665, and 605 K, respectively. Based on PXRD patterns, the types and parameters of the crystal lattices of these compounds were determined. The partial Gibbs free energy, enthalpy, and entropy of bismuth in alloys, standard integral

thermodynamic functions of formation, and standard entropies of bismuth tellurides were calculated from the EMF measurement results.

ACKNOWLEDGEMENTS

The work has been carried out within the framework of the international joint research laboratory “Advanced Materials for Spintronics and Quantum Computing” (AMSQC) established between the Institute of Catalysis and Inorganic Chemistry of ANAS (Azerbaijan) and Donostia International Physics Center (Basque Country, Spain) and partially supported by the Science Development Foundation under the President of the Republic of Azerbaijan, a Grant EIF/MQM/Elm-Tehsil-1-2016-1(26)-71/01/4-M-33.

CONFLICT OF INTEREST

On behalf of all authors, the corresponding author states that there is no conflict of interest.

SUPPLEMENTARY INFORMATION

The online version contains supplementary material available at <https://doi.org/10.1007/s11837-021-04621-1>.

REFERENCES

- N.K. Abrikosov, V.F. Bankina, L.V. Poretskaya, L.E. Shelimova, and E.V. Skudnova, *Semiconducting II–VI, IV–VI, and V–VI Compounds* (Springer, New York, 1969).
- D.M. Rowe, *Thermoelectrics Handbook: Macro to Nano* (CRC, Boca Raton, 2006).
- A.V. Shevelkov, *Russ. Chem. Rev.* 77, 1. <https://doi.org/10.1070/RC2008v077n01ABEH003746> (2008).
- J.W.G. Bos, R.J. Cava, H.W. Zandbergen, M.H. Lee, and N.P. Ong, *Phys. Rev. B* 75, 195203. <https://doi.org/10.1103/PhysRevB.75.195203> (2007).
- I.T. Witting, T.C. Chasapis, F. Ricci, M. Peters, N.A. Heinz, G. Hautier, and G.J. Snyder, *Adv. Electron. Mater.* 5, 1800904. <https://doi.org/10.1002/aeml.201800904> (2019).
- L. Zhao, Y. He, H. Zhang, L. Yi, and J. Wu, *J. Alloys Compd.* 768, 659. <https://doi.org/10.1016/j.jallcom.2018.07.324> (2018).
- J.E. Moore, *Nature* 464, 194. <https://doi.org/10.1038/nature08916> (2010).
- C.L. Kane, and J.E. Moore, *Phys. World* 24, 32. <https://doi.org/10.1088/2058-7058/24/02/36> (2011).
- S.V. Ereemeev, G. Landolt, T.V. Menshchikova, B. Slomski, Y.M. Koroteev, Z.S. Aliyev, M.B. Babanly, J. Henk, A. Ernst, L. Patthey, A. Eich, A.A. Khajetoorians, J. Hagemeister, O. Pietzsch, J. Wiebe, R. Wiesendanger, P.M. Echenique, S.S. Tsirkin, I.R. Amiraslanov, J.H. Dil, and E.V. Chulkov, *Nat. Commun.* 3, 635. <https://doi.org/10.1038/ncomms1638> (2012).
- C. Lamuta, A. Cupolillo, A. Politano, Z.S. Aliiev, M.B. Babanly, E.V. Chulkov, and L. Pagnotta, *Nano Res.* 9, 1032. <https://doi.org/10.1007/s12274-016-0995-z> (2016).
- R. Sultana, P. Neha, R. Goyal, S. Patnaik, and V.P.S. Awana, *J. Magn. Mag. Mater.* 428, 213. <https://doi.org/10.1016/j.jmmm.2016.12.011> (2017).
- A. Lawal, A. Shaari, R. Ahmed, and N. Jarkoni, *Phys. B* 520, 69. <https://doi.org/10.1016/j.physb.2017.05.048> (2017).
- A. Politano, M. Caputo, S. Nappini, F. Bondino, Z.S. Aliiev, M.B. Babanly, and E. Chulkov, *J. Phys. Chem. C* 118, 21517. <https://doi.org/10.1021/jp506444f> (2014).
- C. Lamuta, D. Campi, A. Cupolillo, Z. Aliiev, M. Babanly, E. Chulkov, A. Politano, and L. Pagnotta, *Scr. Mater.* 121, 505. <https://doi.org/10.1016/j.scriptamat.2016.04.036> (2016).
- N.T. Mamedov, E.H. Alizade, Z.A. Jahangirli, Z.S. Aliiev, N.A. Abdulayev, S.N. Mammadov, I.R. Amiraslanov, Y. Shim, K. Wakita, S.S. Ragimov, A.I. Bayramov, M.B. Babanly, A.M. Shikin, and E.V. Chulkov, *J. Vac. Sci. Technol. B* 37, 062602. <https://doi.org/10.1116/1.5122776> (2019).
- P.H. Le, P.T. Liu, C.W. Luo, J. Lin, and K.H. Wu, *J. Alloys Compd.* 692, 972. <https://doi.org/10.1016/j.jallcom.2016.09.109> (2017).
- L. Viti, D. Coquillat, A. Politano, K.A. Kokh, Z.S. Aliiev, M.B. Babanly, O.E. Tereshchenko, W. Knap, E.V. Chulkov, and M.S. Vitiello, L. Viti, *Nano Lett.* 16, 80. <https://doi.org/10.1021/acs.nanolett.5b02901> (2016).
- M.B. Babanly, E.V. Chulkov, Z.S. Aliiev, A. Shevelkov, and I. Amiraslanov, *Russ. J. Inorg. Chem.* 62, 1703. <https://doi.org/10.1134/S00360236171130034> (2017).
- J. Yao, Z. Zheng, and G. Yang, *Adv. Funct. Mater.* 27, 1701823. <https://doi.org/10.1002/adfm.201701823> (2017).
- X. Li, C. Lou, X. Li, Y. Zhang, Z. Liu, and B. Yin, *J. Phys. D* 53, 035102. <https://doi.org/10.1088/1361-6463/ab4edb> (2020).
- Q. Wang, X. Wu, L. Wu, and Y. Xiang, *Aip. Adv.* 9, 025022. <https://doi.org/10.1063/1.5082725> (2019).
- T. Matsushita, and K. Mukai, *Chemical Thermodynamics in Materials Science: From Basics to Practical Applications* (Springer, Singapore, 2018).
- R. DeHoff, *Thermodynamics in Materials Science*, 2nd edn. (CRCs, Boca Raton, 2006).
- M.B. Babanly, L.F. Mashadiyeva, D.M. Babanly, S.Z. Imamaliyeva, D.B. Taghiyev, and Y.A. Yusibov, *Russ. J. Inorg. Chem.* 64, 1649. <https://doi.org/10.1134/S0036023619130035> (2019).
- M. Hansen, and K. Anderko, *Constitution of Binary Alloys*, 2nd edn. (McGraw-Hill, New York, 1958).
- A. Brown, and B. Lewis, *J. Phys. Chem. Solids* 23, 1597. [https://doi.org/10.1016/0022-3697\(62\)90242-1](https://doi.org/10.1016/0022-3697(62)90242-1) (1962).
- N.K. Abrikosov, and V.F. Bankina, *Russ. J. Inorg. Chem.* 3, 659. (1958).
- A.C. Glatz, A.C. Glatz, *J. Electrochem. Soc.* 112, 1204. <https://doi.org/10.1149/1.2423400> (1965).
- M.M. Stasova, M.M. Stasova, *Zh. Strukt. him.* 8(4), 584. (1967).
- E.M. Imamov, and S.A. Semiletov, *Sov. Phys. Crystallogr.* 15(5), 845. (1971).
- R.F. Brebrick, *The Chemistry of Extended Defects in Non-metallic Solids*, 1st edn. (Elsevier, Amsterdam, 1970), pp 183–197.
- R.F. Brebrick, *J Appl. Crystallogr.* 1, 241. <https://doi.org/10.1107/S0021889868005406> (1968).
- K. Okamoto, and L.E. Tanner, Bi–Te (bismuth–tellurium), in *Binary Alloy Phase Diagrams*. ed. by T.B. Massalski, and K. Ohamoto (ASM International, Materials Park, 1990), p. 800.
- L.E. Shelimova, O.G. Karpinsky, V.I. Kosyakov, V.A. Sheshtakov, V.S. Zemskov, and F.A. Kuznetsov, *J. Struct. Chem.* 41, 81. <https://doi.org/10.1007/BF02684732> (2000).
- C. Mao, M. Tan, L. Zhang, D. Wu, W. Bai, and L. Liu, *Calphad* 60, 81. <https://doi.org/10.1016/j.calphad.2017.11.007> (2018).
- W. Gierlotka, *Calphad* 63, 6. <https://doi.org/10.1016/j.calphad.2018.08.005> (2018).
- Data base of thermal constants of substances*. Digital version, Eds. V.S. Iorish and V.S. Yungman. (2006) <http://www.chem.msu.ru/cgi-bin/tkv.pl?show=welcome.html>.
- O. Kubaschewski, C.B. Alcock, and P.J. Spenser, *Materials Thermochemistry* (Pergamon, London, 1993).
- I. Barin, *Thermochemical Data of Pure Substances*, 3rd edn. (Wiley-VCH, New York, 2008).
- K.C. Mills, *Thermodynamic Data for Inorganic Sulphides Selenides and Tellurides* (Butterworth, London, 1974).
- V.R. Sidorko, L.V. Goncharuk, and R.V. Antonenko, *Powder Metall. Metal. C+* 47, 234. <https://doi.org/10.1007/s11106-008-9009-3> (2008).
- B.T. Melekh, and S.A. Semenkovich, *Izv. AN SSSR. Neorg. Mater.* 4, 1346. (1968).
- B.W. Howlett, S. Misra, and M.B. Bever, *Trans. Metall. Soc. AIME* 230, 1367. (1964).
- A.A. Vecher, L.A. Mechkovskii, and A.S. Skoropanov, *Izv. AN SSSR. Neorg. Mater.* 10, 2140. (1974).
- Z. Boncheva-Mladenova, A.S. Pashinkin, and A.V. Novoselova, *Izv. AN SSSR. Neorg. Mater.* 4, 291. (1968).
- A.F. Zurhelle, V.L. Deringer, R.P. Stoffel, and R. Dronskowski, *J. Phys-Condens. Mater.* 28, 115401. <https://doi.org/10.1088/0953-8984/28/11/115401> (2016).
- G. Morgant, Y. Feutelais, B. Legendre, R. Castanet, and A. Coulet, *Z. Metallk.* 81, 44. (1990).
- G.S. Hasanova, G.B. Dashdiyeva, Y.A. Yusibov, and M.B. Babanly, *Chem. Probl.* 3, 315. (2020).
- G.S. Hasanova, A.T. Mammadova, A.I. Aghazade, S.Z. Imamaliyeva, and M.B. Babanly, Refinement of the phase diagram of the bi-se system and thermodynamic properties of the bismuth selenides, in *XII International conference "Electronic Processes in organic and Inorganic Materials", Ukraine, 2020*, p. 209.
- C. Wagner, *Thermodynamics of Alloys*, 1st edn. (Addison-Wesley, Boston, 1952).
- A.G. Morachevsky, G.F. Voronin, V.A. Geyderich, and I.B. Kutsenok, *Electrochemical research methods in the thermodynamics of metallic systems* (Akademkniga, Moscow, 2003) **(in Russian)**.
- M.B. Babanly, Y.A. Yusibov, and N.B. Babanly, in *Electromotive Force and Measurement in Several Systems*. ed. by S. Kara, (Intechweb.Org, 2011).
- M. Moroz, F. Tesfaye, P. Demchenko, M. Prokhorenko, and D. Lindberg, *J. Electron. Mater.* 47, 5433. <https://doi.org/10.1016/j.solidstatesciences.2020.106344> (2018).

54. M. Moroz, F. Tesfaye, P. Demchenko, M. Prokhorenko, Y. Kogut, O. Pereviznyk, S. Prokhorenko, and O. Reshetnyak, *Solid State Sci.* 107, 106344. <https://doi.org/10.1016/j.solidstatesciences.2020.106344> (2020).
55. N.B. Babanly, E.N. Orujlu, S.Z. Imamaliyeva, Y.A. Yusibov, and M.B. Babanly, *J. Chem. Thermodyn.* 128, 78. (2019).
56. N.B. Babanly, S.Z. Imamaliyeva, Y.A. Yusibov, D.B. Taghiyev, and M.B. Babanly, *J. Solid State Electrochem.* 22, 1143. <https://doi.org/10.1007/s10008-017-3853-3> (2018).
57. I. Dzh, S.Z. Alverdiev, D.M. Imamaliyeva, Yu.A. Babanly, D.B.T. Yusibov, and M.B. Babanly, *Russ. J. Electrochem.* 55, 467. <https://doi.org/10.1134/S1023193519050021> (2019).
58. V. Vassiliev, and W. Gong, in *New Advances in Fundamental Researches and Applications*. ed. by Y. Shao, (IntechOpen, 2012), p. 71. <https://doi.org/10.5772/39007>.
59. E.G. Osadchii, Y.I. Korepanov, and N.N. Zhdanov, *Instrum. Exp. Tech.* 59, 302. <https://doi.org/10.1134/S0020441216010255> (2016).
60. S.Z. Imamaliyeva, I.F. Mekhdiyeva, D.M. Babanly, V.P. Zlomanov, D.B. Tagiyev, and M.B. Babanly, *Russ. J. Inorg. Chem.* 65, 1762. <https://doi.org/10.1134/S0036023620110066> (2020).
61. S.Z. Imamaliyeva, D.M. Babanly, T.M. Gasanly, and D.B. Tagiev, *Russ. J. Phys. Chem. A* 92, 2111. <https://doi.org/10.1134/S0036024418110158> (2018).
62. M.V. Prokhorenko, M.V. Moroz, and P.Y. Demchenko, *Russ. J. Phys. Chem. A* 89, 1330. <https://doi.org/10.1134/S0036024415080269> (2015).
63. F. Tesfaye, M. Moroz, O. Reshetnyak, D. Lindberg, P. Taskinen, and L. Hupa, in *Thermophysical Properties of Complex Materials*. ed. by A. Shahzad, (IntechOpen, 2019), p. 1. <https://doi.org/10.5772/intechopen.86878>.
64. Z.S. Aliev, S.S. Musayeva, S.Z. Imamaliyeva, and M.B. Babanly, *J. Therm. Anal. Calorim.* 133, 1115. <https://doi.org/10.1007/s10973-017-6812-4> (2018).
65. S.Z. Imamaliyeva, S.S. Musayeva, D.M. Babanly, Y.I. Jafarov, D.B. Tagiyev, and M.B. Babanly, *Thermochim. Acta* 679, 178319. <https://doi.org/10.1016/j.tca.2019.178319> (2019).
66. E. Zavyalov, V. Begizov, and G. Nechelyustov, *Dokl. Akad. Nauk SSSR* 230, 1439. ((in Russian)) (1976).
67. K. Yamana, K. Kihara, and T. Matsumoto, *Acta Crystallogr. Sec. B* 35, 147s. (1979).

Publisher's Note Springer Nature remains neutral with regard to jurisdictional claims in published maps and institutional affiliations.